Temporal and Spatial Dynamics of Subsidence in Eastern Jharia, India

Aditya Kumar Thakur[1], Luvkesh Attri[2], Rahul Dev Garg[1], Kamal Jain[1], Dheeraj Kumar[3], Arnab Chowdhury[1]

[1]Department of Civil Engineering, Indian Institute of Technology Roorkee, Roorkee, India - aditya_kt@ce.iitr.ac.in; rdgarg@ce.iitr.ac.in; kamal.jain@ce.iitr.ac.in; arnab_c@ce.iitr.ac.in
[2]Department of Civil Engineering, Indian Institute of Technology Bombay, Mumbai, India – 23d0273@iitb.ac.in
[3]Department of Mining Engineering, Indian Institute of Technology (Indian School of Mines) Dhanbad, India - dheeraj@iitism.ac.in

Keywords: Jharia Coalfield, Subsidence, Sentinel-1, Seasonal Deformation, Time-series Analysis.

Abstract

Jharia, one of the oldest and most significant mining areas, is facing the issue of subsidence for different reasons, such as coal fires, underground mining, and soil sensitivity towards seasonal change. This paper concentrates on the subsidence analysis of the Eastern region of the Jharia Coalfield from January 2018 to January 2021. Sentinal-1 SLC SAR imagery is used for multi-image sparse point processing and generating time series. Data processing is done using SARPROZ software. Further, the PS points inside the study area are filtered, and a classification map is drawn using ArcGIS software. The yearly percentage change of different classified zones is examined. The percentage change is significant for subsiding and uplifting zones but minimal for stable zones. Different critically and highly subsiding areas are identified by overlaying the classification zones on the topographic map. The seasonal variation of cumulative displacement is also examined, and patterns are analyzed. Different regions have different sensitivity towards seasonal variation. Overall, this paper provides insightful deformation results over Eastern Jharia for 2018-2021.

1. Introduction

Jharia Coalfield, located in the Dhanbad district of Jharkhand, India, is one of the country's oldest and most significant coal mining areas. The area is prone to coal fire and subsidence, which makes the region critical, and hence continuous monitoring is required. Many approaches have been made in recent years to study surface and subsurface fires and induced mining and fire subsidence. In a study, the Jharia Coalfield's subsurface coal fires were monitored using Differential Interferometry Synthetic Aperture Radar (DInSAR), which revealed that the eastern and western borders were the main locations of coal fire-related subsidence. Based on the ground subsidence result, it forecasted probable areas for coal fires (Gupta et al., 2013). A study of dynamic active and residual subsidence in the Jharia Coalfield suggests that the mining rate is crucial in determining subsidence rates. Their inter-relationship showed a rational trend. However, a poor association between compressive and tensile strains, slope, and rate of face advance is observed (Prakash et al., 2014).

Use of C and L-bands DInSAR, GPS, and precision levelling techniques for subsidence assessment discovered previously unreported subsidence sites. C-band DInSAR indicated slowly subsiding areas, while L-band found rapidly subsiding areas. C-band DInSAR was demonstrated to be more sensitive to slow deformation than L-band (Chatterjee et al., 2015). Another study identified the sinking areas in Jharia Coalfield using the Radarsat-2 C-band data. They created a land subsidence map using InSAR to identify new subsidence locations. 6.9 sq km of fresh subsidence zones were found. Based on the subsidence rates, regions susceptible to roof collapse were also identified (Chatterjee et al., 2016).

The Sarscape program generates interferograms for DInSAR analysis, which is used to detect subsidence. ALOS PALSAR data can efficiently identify areas of moderate to rapid subsidence. Fringes from interferograms are superimposed on images to locate subsidence. Subsidence rates range from 7.88 cm/year to 56.72 cm/year, with a total impacted area of 7.2 square kilometres observed (Borah et al., 2017). Factors causing subsidence in Jharia Coalfields were explored using statistical approaches involving factor analysis, principal component analysis, and cluster analysis for evaluation. It identified two essential components contributing to subsidence variability: natural causes and subsidence coefficients, which account for 42.327% and 24.661%, respectively (Sahu et al., 2017).

The Small Baseline Subset (SBAS) approach was used on 23 X-band COSMO-SKyMed (CSK) datasets from 2011 to 2016 to determine the annual subsidence rate over the Jharia Coal Field. Using groundwater level data, validating subsidence results shows that underground coal mining mainly causes surface deformation in the Jharia area. Grey Relational Analysis (GRA) can demonstrate quantitative similarities between surface subsidence and groundwater level change patterns (Dey et al., 2019). A study used modified PS-InSAR and C-band SAR data for land subsidence mapping, focusing on detecting gradual surface deformation due to coal mining activities. The methodology identifies continual slow rate subsidence at five primary sites. The Alkusa location shows a higher rate of subsidence. The highest rate of gradual deformation observed is 29 mm/year (Kumar et al., 2020).

The impact of coal fire on subsidence was investigated in Jharia Coalfield, which employs satellite data for hazard mapping and subsidence quantification. A strong positive association between subsidence velocity and temperature anomaly has been established. A maximum subsidence of 20 cm/year and temperature anomalies of up to 25°C were observed. Kusunda, Keshalpur, and Bararee collieries have been designated as critically damaged areas that require immediate assistance (Karanam et al., 2021). Surface deformation time-series analysis from 2017 to 2020 using the N-SBAS technique successfully maps the 9.5 sq km coal fire region. Tisra, Chhatatanr, and Sijua were among the towns classified as

vulnerable. Kusunda colliery had the highest coal fire activity, with 22 cm of subsidence. The integration of dense SAR datasets resulted in a credible surface deformation map (Riyas et al., 2021).

Satellite data was used to analyse temperature anomalies and ground deformation to track subsurface fires. Land surface temperature and subsidence sites were mapped to detect ground deformation and thermal anomaly patterns in the Jharia coal mine. InSAR data was combined with thermal anomalies to track underground coal mine fires (Kim et al., 2021). Another study determined displacement, land surface temperature, and subsidence types in relation to coal fire-induced land subsidence in Jharia Coalfield, using satellite data. The displacement rate varied at active mine benches and overburden dumps, as evidenced by thermal anomalies and patterns of subsidence associated with coal fires. In the study area, deformation and thermal anomalies were found to be closely associated (Raju and Mehdi, 2023).

In all the previous research, the approach to studying subsidence overlooks zone classification, area identification, and seasonal variation. In this study, a subsidence analysis of the eastern region of the Jharia Coalfield was done from January 2018 to January 2021. The area prone to subsidence was calculated using a reclassification map for the same period. The subsidence zones were identified, and yearly change analysis was done for different regional subsiding and uplifting zones. Different areas prone to subsidence were identified by overlapping the zones on the topographic map. The seasonal deformation change was also estimated, and the change pattern was determined. Overall, this study highlighted the change analysis of subsiding and uplifting zones and seasonal variation of cumulative displacement over the eastern region of Jharia Coalfield.

2. Study Area

Jharia Coalfield is the largest Coalfield near the city of Dhanbad in India, yielding a large amount of coal every year to fulfil the country's coal demand (Dutta Dey and Singh, 2021). The continuous burning coalfield of Jharia spans about 450 sq km having a latitudinal and longitudinal spread of 23.58°N to 23.91°N and 86.08°E to 86.55°E, respectively. The region is heavily impacted by many coal fires every year (Singh et al., 2021). The area is on the Damodar River valley, covered by the Damuda Group of the lower Gondwana Formation (Biswal and Gorai, 2020). Metamorphic rocks from the Archaean period serve as a formation of the Jharia Coalfield's basement. The Barakar Formation, which contains several coal seams, is the most significant geological unit in the region. Barakars covers eighteen major workable coal seams. Coking coal is the most abundant among them. The area includes carbonaceous shales, pebbly sandstone, and shales (Verma et al., 1979). We analysed the subsidence of east Jharia in this study (Figure 1), which includes Nayadih, Bhagatdih, Kustore, Bhagarampur, Tisra and Suranga areas of the Dhanbad district. The latitudinal and longitudinal extensions of our study area are 23.682°N to 23.788°N and 86.362°E to 86.461°E, respectively, having an area of 67.93 sq km.
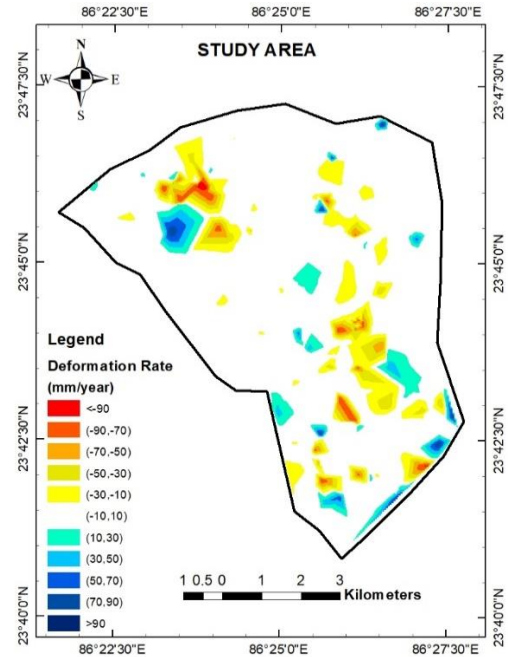

Figure 1. Map showing the extent of the study area with deformation rate from January 2018 to January 2021.

3. Methodology

3.1 Dataset

We used the Sentinel-1 as the SAR dataset in this study. Sentinel-1 is a radar satellite mission designed by the European Space Agency (ESA) under the Copernicus program. It is outfitted with C-band synthetic aperture radar (SAR) technology, allowing it to observe the Earth's surface regardless of weather, cloud coverage, or time of day. The C-band radar has a wavelength of around 5.6 cm. It provides moderate-resolution imaging suited for various applications, including Earth surface monitoring, maritime surveillance, environmental, agricultural, glacier and ice sheet monitoring, etc. Sentinel-1 is a constellation of two satellites, Sentinel-1A and Sentinel-1B, that work together to give global coverage in six days or less. This frequent revisit time is critical for constantly monitoring dynamic events on the Earth's surface.

3.2 Software

SARPROZ provides a user-friendly graphical interface and offers tools for processing SAR data and generating interferograms, which are images that illustrate the phase difference between two SAR acquisitions. This enables users to detect ground deformations such as subsidence and uplift. The software allows you to generate and analyse time-series interferograms, which enables you to track surface deformation over long periods. It also makes it easier to analyse various SAR images collected over time, allowing users to investigate temporal trends in ground motion.

Esri developed ArcGIS, a Geographic Information System (GIS) software platform. It offers a full set of tools for managing, analysing, and visualising spatial data. ArcGIS is widely used by businesses and individuals for a wide range of applications,

including urban planning, natural resource management, environmental monitoring, disaster response, and much more. The software can be used for mapping and visualisation, data management, spatial analysis, geocoding, and geolocation, among other tasks.
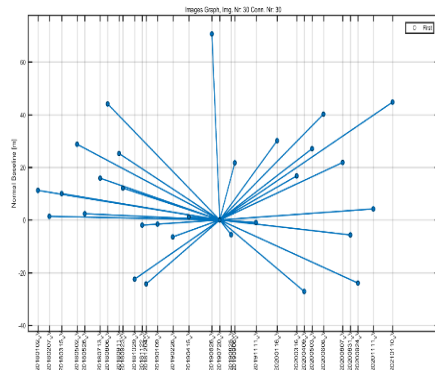
3.3 Processing

Figure 2. The normal baseline of SLC images used for generating interferograms.
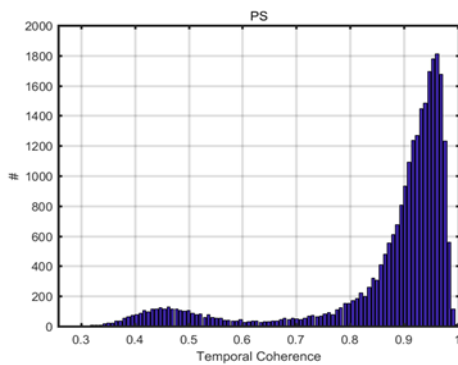

Figure 3. Temporal coherence of different PS (Permanent Scatterers) points of acquired images

In the present study, 30 SLC images from Sentinel-1 (C-band) were used to generate the interferograms, covering dates from January 2018 to January 2021. The sentinel data processing (Figure 4) is done using SARPROZ software. During processing, the image acquired on 27th July 2019 was selected as the master image (Figure 2) for generating interferograms and identifying stable points for further analysis. The different PS points have different temporal coherence (Figure 3). The built-up area showed a higher coherence value than the mining, agriculture and forest areas. Coherence loss is also seen in open-cast mines due to continuous mining activity. A network of PS points was generated based on the Amplitude Stability Index of 0.75, denoting the point targets whose amplitude was least affected by the decorrelation effects that occurred in the study area. Finally, we obtained 2345 points reflecting the deformation in the study area. Then, we used TIN (Triangulated Irregular Network) interpolation on the ArcMap platform to create 4665 triangles representing the reclassified subsidence map of the Jharia Coalfield. It is basically a vector representation of the interpolated surface created from the obtained points.
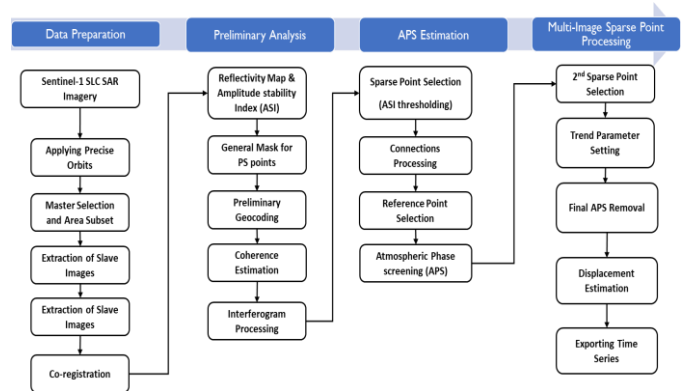

Figure 4. Flowchart of Sentinal-1 data processing

4. Results and Discussions

4.1. Zone division

From ArcGIS, the data points were processed for different years. Table 1 shows the area under different subsidence and uplifting intervals. We can observe the zonal shifting of subsidence and upliftment from year to year, i.e. from high to low or low to high subsidence and upliftment. The % change in subsiding and uplifting regions was significant, while the % change in the stable zones was almost negligible.

Table 1. Table showing the % change in the areas of different subsidence and uplifting zones in three consecutive years (2018, 2019, and 2020). The subsidence values are categorized based on the subsidence rate (yearly subsidence).

| Def. rate (cm/year)	Area (sq.km.)			% change in area	
	2018	2019	2020	2018-19	2019-20
<-11	0.00021	0.00006	0.00000	-69.8	-100
(-11,-9)	0.06649	0.08777	0.03529	32.0	-59.8
(-9,-7)	0.44126	0.34834	0.37226	-21.1	6.9
(-7,-5)	0.89712	0.86350	0.87117	-3.8	0.9
(-5,-3)	1.85236	1.88406	1.76043	1.7	-6.6
(-3,-1)	6.21209	5.50960	4.80941	-11.3	-12.7
(-1,1)	51.29128	52.36316	52.66901	2.1	0.6
(1,3)	4.33077	4.06506	4.51520	-6.1	11.1
(3,5)	1.71455	1.67618	1.71666	-2.2	2.4
(5,7)	0.86123	0.85304	0.86296	-1.0	1.2
(7,9)	0.247070	0.26965	0.30021	9.1	11.3
>9	0.01557	0.00956	0.01737	-38.6	81.6

4.2. Critical Subsiding Zone
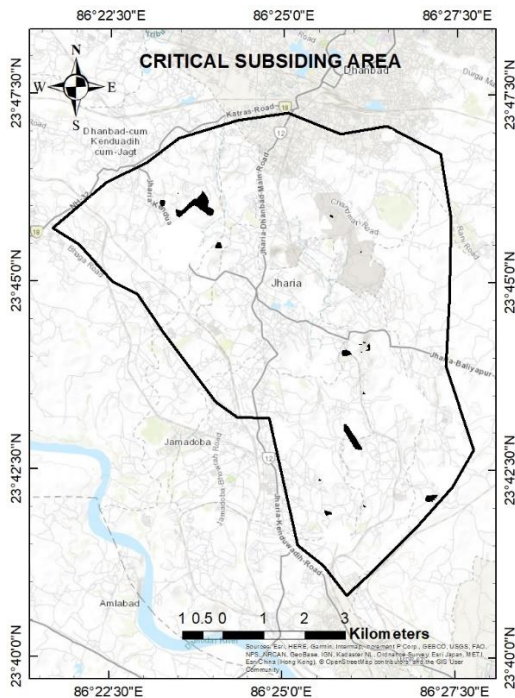
Figure 5. Critical Subsiding Zone

The critical subsiding zone (Figure 5) is considered to have an average subsidence greater than 7cm/year for three consecutive years. In the study area, 0.44 sq. km. of area falls under this region. This region shows rapid subsidence (Figure 6) and is the most hazardous zone. Some of the locations and their coordinates around which critical subsiding zones are identified are:

1. Over dump of the Alkusa opencast mines, east of Shankar road (23.767N,86.396E)
2. Ena colliery opencast mines, east of Shankar road, Bhagatdih (23.758N,86.401E)
3. 300 m west of Kali Mandir , B.R. company Jayrampur colliery, Tisra (23.715N,86.434E)
4. 1km east of Jeenagora BCCL hospital, Tisra (23.702N,86.452E)
5. 400m north of Kuzama Kali Mandir, Tisra (23.734N,86.432E)
6. 200m south of Begariya more, Bararee Road, Jorapokhar, (23.699N,86.427E)
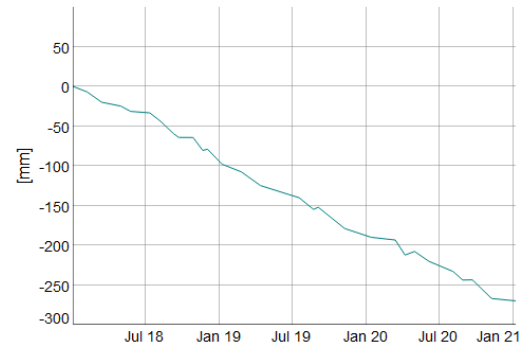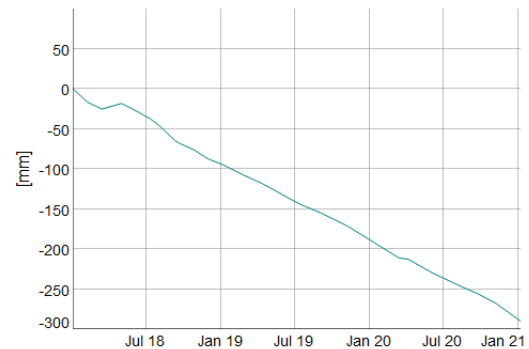

Figure 6. Temporal variation of Cumulative displacement of Point under Critical Subsiding Zone
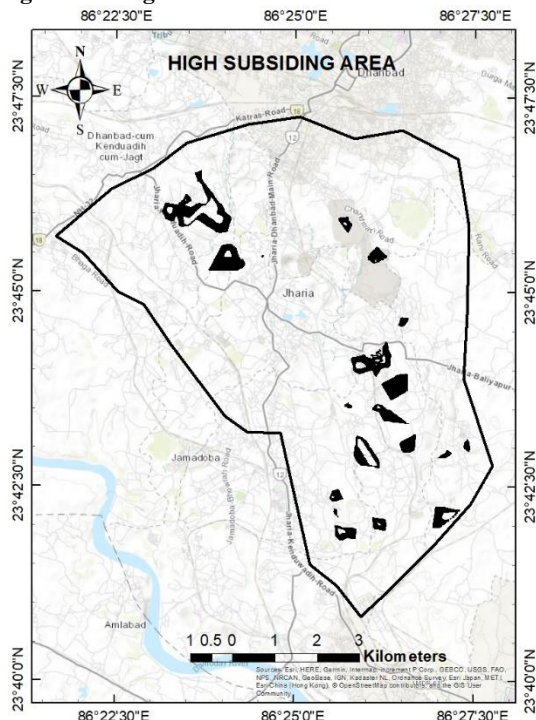
4.3. High Subsiding Zone

Figure 7. High Subsidence zone

The high subsiding zone (Figure 7) has an average subsidence between 3cm/year and 7cm/year for three consecutive years. In the study area, 2.78 sq. km. of area falls under this region. This region also shows a high value of subsidence (figure 8) but is comparatively lesser than the critical zone and can be considered a hazardous zone. All the zones periphery to Critical Subsiding Zone falls under high subsiding area. Some more locations and their coordinates around which high subsiding zones are identified are:

1. 100m south of Bank of India, Lodna or Near Dev Group, Tisra (23.729N,86.441E)
2. 500m north-east of Jayrampur Goverment School, Tisra (23.717N,86.443E)
3. 200m north of Dobari Opencast Mine BCCL, Bera (23.758N,86.435E)
4. 500m east of Lodna colliery high school, Lodna (23.724N,86.438E)
5. North side of Ena colliery opencast mines, Bhagatdih (23.757N,86.400E)

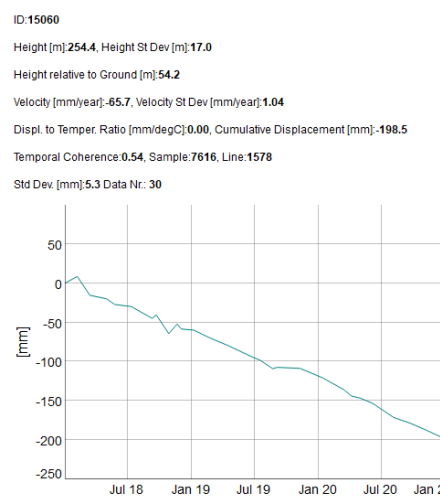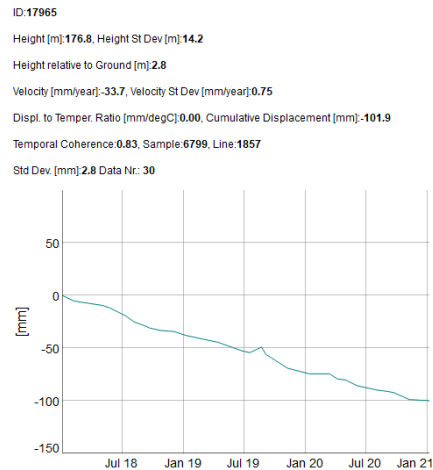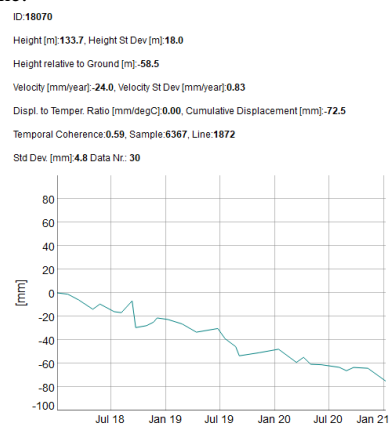Figure 8. Temporal variation of Cumulative displacement of Points under High Subsiding Zone

4.4. Moderate Subsiding Zone

The moderate subsiding zone has an average subsidence between 1cm/year and 3cm/year for three consecutive years. In the study area, 5.18 sq. km. of area falls under this region. This region shows a low value of subsidence (Figure 9) and can be considered a low hazardous zone.
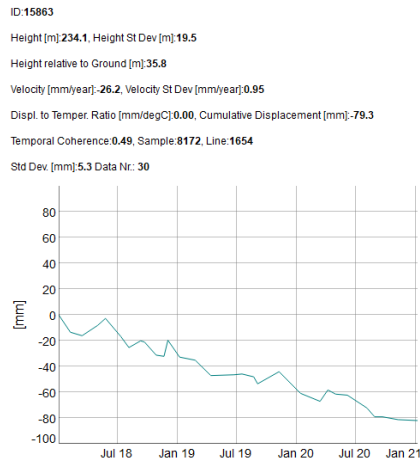
ID:15863
Height [m]:**234.1**, Height St Dev [m]:**19.5**
Height relative to Ground [m]:**35.8**
Velocity [mm/year]:**-26.2**, Velocity St Dev [mm/year]:**0.95**
Displ. to Temper. Ratio [mm/degC]:**0.00**, Cumulative Displacement [mm]:**-79.3**
Temporal Coherence:**0.49**, Sample:**8172**, Line:**1654**
Std Dev. [mm]:**5.3** Data Nr.: **30**

Figure 9. Temporal variation of cumulative displacement of Points under the Moderate subsiding Zone

4.5. Stable Zone

The stable zone has an average subsidence and upliftment between -1cm/year and 1cm/year, respectively, for three consecutive years. Most of the area under the Jharia Coalfield is in a stable zone. In the study area, 55.74 sq. km. of area falls under this region. Some regions inside this zone show linear (Figure 10), whereas some regions show zig-zag patterns (Figure 11) of cumulative displacement curve with respect to time, highlighting the area's sensitivity to seasonal change. Very low subsiding area (figure 11) and very low uplifting area (Figure 12) also came under the stable zone.
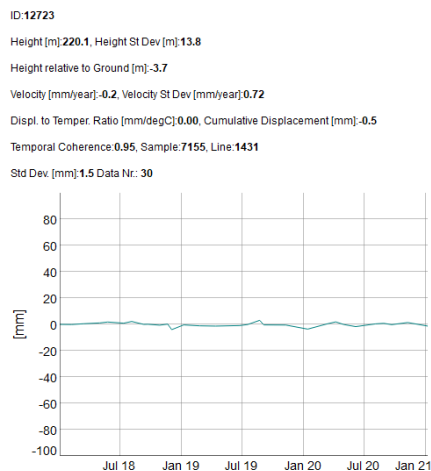

ID:**12723**
Height [m]:**220.1**, Height St Dev [m]:**13.8**
Height relative to Ground [m]:**-3.7**
Velocity [mm/year]:**-0.2**, Velocity St Dev [mm/year]:**0.72**
Displ. to Temper. Ratio [mm/degC]:**0.00**, Cumulative Displacement [mm]:**-0.5**
Temporal Coherence:**0.95**, Sample:**7155**, Line:**1431**
Std Dev. [mm]:**1.5** Data Nr.: **30**

Figure 10. Temporal variation of Cumulative displacement of Point under Stable Zone

ID:**14398**
Height [m]:**243.6**, Height St Dev [m]:**15.1**
Height relative to Ground [m]:**36.6**
Velocity [mm/year]:**-5.3**, Velocity St Dev [mm/year]:**0.93**
Displ. to Temper. Ratio [mm/degC]:**0.00**, Cumulative Displacement [mm]:**-16.1**
Temporal Coherence:**0.55**, Sample:**7311**, Line:**1526**
Std Dev. [mm]:**5.0** Data Nr.: **30**
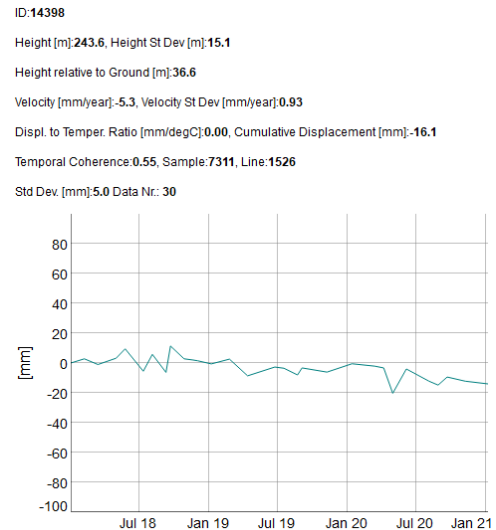
Figure 11. Temporal variation of Cumulative displacement of Point under Stable Zone showing Seasonal Effect

ID:**16776**
Height [m]:**177.8**, Height St Dev [m]:**13.7**
Height relative to Ground [m]:**-3.1**
Velocity [mm/year]:**5.5**, Velocity St Dev [mm/year]:**0.73**
Displ. to Temper. Ratio [mm/degC]:**0.00**, Cumulative Displacement [mm]:**16.6**
Temporal Coherence:**0.97**, Sample:**7937**, Line:**1743**
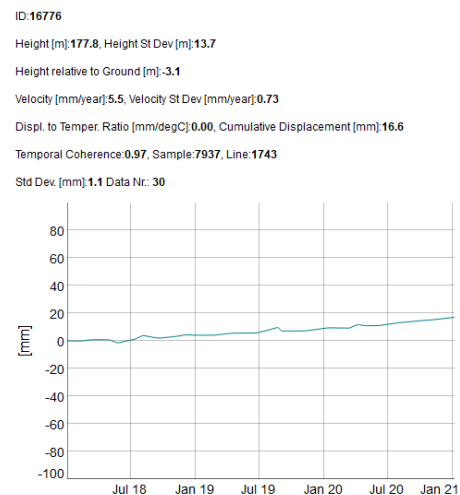Std Dev. [mm]:**1.1** Data Nr.: **30**

Figure 12. Temporal variation of Cumulative displacement of Point under Stable Zone showing very low-rate gradual upliftment

4.6. Uplifting Zone

The uplifting zone has an average upliftment greater than 1cm/year for three consecutive years. In the study area, 3.79 sq. km. of area falls under this region. This zone can be further classified as low (Figure 13), moderate (Figure 14) and high upliftment zone (Figure 15) based on the rate of upliftment.
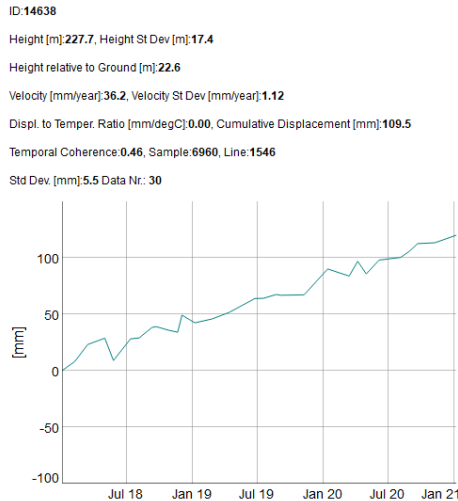
ID:14638

Height [m]:227.7, Height St Dev [m]:17.4

Height relative to Ground [m]:22.6

Velocity [mm/year]:36.2, Velocity St Dev [mm/year]:1.12

Displ. to Temper. Ratio [mm/degC]:0.00, Cumulative Displacement [mm]:109.5

Temporal Coherence:0.46, Sample:6960, Line:1546

Std Dev. [mm]:5.5 Data Nr.: 30

Figure 13. Temporal variation of Cumulative displacement of Point under Low Uplifting Zone

ID:13641

Height [m]:314.6, Height St Dev [m]:15.0

Height relative to Ground [m]:104.8

Velocity [mm/year]:76.6, Velocity St Dev [mm/year]:1.34

Displ. to Temper. Ratio [mm/degC]:0.00, Cumulative Displacement [mm]:231.5

Temporal Coherence:0.46, Sample:6964, Line:1476

Std Dev. [mm]:5.9 Data Nr.: 30
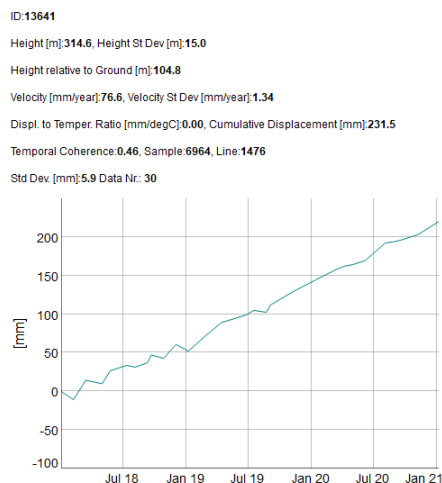
Figure 14. Temporal variation of Cumulative displacement of Point under Moderate Uplifting Zone.

ID:14975

Height [m]:318.9, Height St Dev [m]:40.2

Height relative to Ground [m]:104.8

Velocity [mm/year]:91.0, Velocity St Dev [mm/year]:1.01

Displ. to Temper. Ratio [mm/degC]:0.00, Cumulative Displacement [mm]:275.0

Temporal Coherence:0.48, Sample:6965, Line:1573

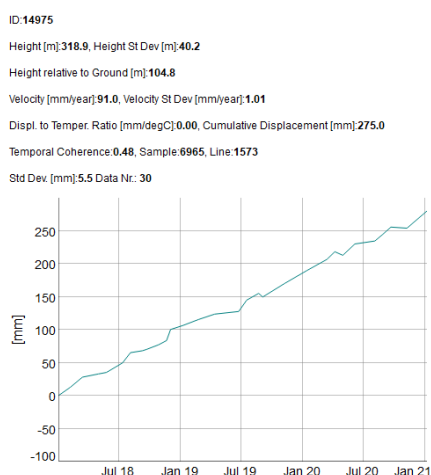Std Dev. [mm]:5.5 Data Nr.: 30

Figure 15. Temporal variation of Cumulative displacement of Point under High Uplifting Zone

4.7. Seasonal Upliftment and Subsidence

The seasonal upliftment and subsidence were analyzed by plotting the subsidence curve at 36-day intervals and calculating the coefficient of determination for a linear trendline. A coefficient of determination value close to one indicates a zone not prone to seasonal upliftment and subsidence, whereas a low value suggests susceptibility to these changes. Significant variations were observed mainly from May to September, corresponding to the monsoon season, as shown in Figures 9, 11, and 13. During this period, soil swelling occurs due to water infiltration, which slows down the normal subsidence rate and increases the upliftment rate.

Conversely, during summer period, the soil tends to shrink or sink, reversing the trend observed during the monsoon season. This alternating pattern of swelling and sinking was also reflected in the cumulative displacement variations shown in Figure 17. The cumulative displacement curves exhibited similar patterns of swelling and sinking across different samples at the same acquisition times, indicating that seasonal moisture variations significantly impact soil behavior.
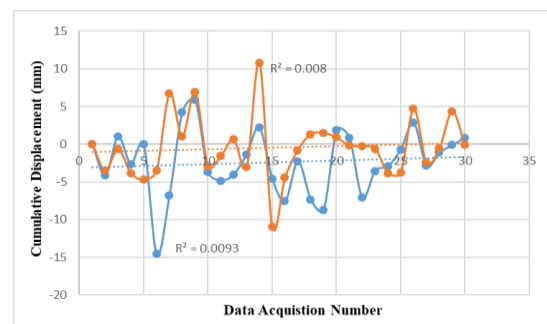

Figure 16. Comparison of Cumulative Displacement of two Stable Points at different Acquisition numbers.
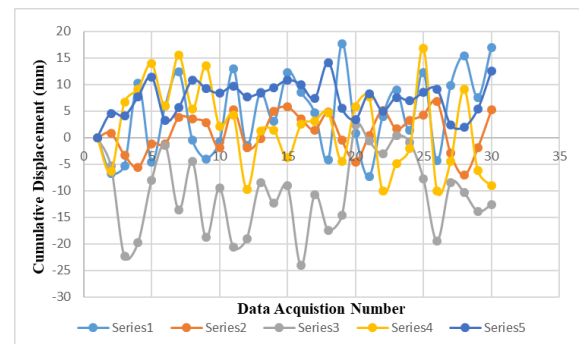

Figure 17. Pattern of Cumulative Displacement of different Stable Points at different Acquisition numbers.

5. Conclusion

In this study, East Jharia was classified into different subsiding, stable, and uplifting zones. The locations identified as critical subsiding zone are: over dump of the Alkusa opencast mines in the east of Shankar road, Ena colliery opencast mines, in Bhagatdih, 300 m west of Kali Mandir of B.R. company Jayrampur colliery in Tisra, 1km east of Jeenagora BCCL hospital in Tisra, 400m north of Kuzama Kali Mandir in Tisra and 200m south of Begariya more Bararee Road in Jorapokhar. These areas are near open-cast mines

or in between the different mining boundaries. Further, the areas identified under the high subsiding zone are:100m south of Bank of India Lodna in Tisra, 500m north-east of Jayrampur Goverment School in Tisra, 200m north of Dobari Opencast Mine BCCL in Bera, 500m east of Lodna colliery high school and North side of Ena colliery opencast mines in Bhagatdih. Along with these areas, the periphery of the critically subsiding zones showed a high subsidence value.

Further, the study of the dynamics of different zones showed a significant change in the area of different subsiding and uplifting zones, where the percentage change in stable zones was very low. The study of the seasonal effect of cumulative displacement showed that different areas have different sensitivity towards seasonal change. The deformation patterns of different points were also analysed, which showed similar dynamics. Significant change was observed during the months of May to September. Overall, this research provided valuable insight into the subsidence phenomena of the eastern Jharia Coalfield. However, more detailed analysis is needed in this field on the correlation of subsidence and soil swelling and sinking, rainfall duration, monsoon timing, etc.

Acknowledgement

References

Biswal, S.S., Gorai, A.K., 2020. Change detection analysis in coverage area of coal fire from 2009 to 2019 in Jharia Coalfield using remote sensing data. *Int. J. Remote Sens.* 41, 9545–9564. https://doi.org/10.1080/01431161.2020.1800128

Borah, S.B., Chatterjee, R.S., Thapa, S., 2017. Detection of underground mining induced land subsidence using Differential Interferometric SAR (D- InSAR) in Jharia Coalfields. *ADBU-Journal Eng. Technol. Detect.* 6, 72–77.

Chatterjee, R.S., Singh, K.B., Thapa, S., Kumar, D., 2016. The present status of subsiding land vulnerable to roof collapse in the Jharia Coalfield, India, as obtained from shorter temporal baseline C-band DInSAR by smaller spatial subset unwrapped phase profiling. *Int. J. Remote Sens.* 37, 176–190. https://doi.org/10.1080/2150704X.2015.1126376

Chatterjee, R.S., Thapa, S., Singh, K.B., Varunakumar, G., Raju, E.V.R., 2015. Detecting, mapping and monitoring of land subsidence in Jharia Coalfield, Jharkhand, India by spaceborne differential interferometric SAR, GPS and precision levelling techniques. *J. Earth Syst. Sci.* 124, 1359–1376. https://doi.org/10.1007/s12040-015-0606-5

Dey, T.K., Biswas, K., Chakravarty, D., Misra, A., Samanta, B., 2019. SPATIO-TEMPORAL SUBSIDENCE ESTIMATION OF JHARIA COAL FIELD , INDIA USING SBAS-DINSAR WITH COSMO-SKYMED DATA Department of Mining Engineering , Indian Institute of Technology Kharagpur , India Advanced

Technology Development Centre , Indian Institute of Te. IGARSS 2019 - 2019 *IEEE Int. Geosci. Remote Sens. Symp.* 2123–2126.

Dutta Dey, S., Singh, R., 2021. Mapping precarious energy geographies: Exploring the lived experience of coal mining in Jharia, India. *Energy Res. Soc. Sci.* 82, 102298. https://doi.org/10.1016/j.erss.2021.102298

Gupta, N., Syed, T.H., Athiphro, A., 2013. Monitoring subsurface coal fires in Jharia Coalfield using observations of land subsidence from differential interferometric synthetic aperture radar (DInSAR). *J. Earth Syst. Sci.* 122, 1249–1258. https://doi.org/10.1007/s12040-013-0355-2

Karanam, V., Motagh, M., Garg, S., Jain, K., 2021. Multi-sensor remote sensing analysis of coal fire induced land subsidence in Jharia Coalfields, Jharkhand, India. *Int. J. Appl. Earth Obs. Geoinf.* 102, 102439. https://doi.org/10.1016/j.jag.2021.102439

Kim, J., Lin, S.Y., Singh, R.P., Lan, C.W., Yun, H.W., 2021. Underground burning of Jharia coal mine (India) and associated surface deformation using InSAR data. *Int. J. Appl. Earth Obs. Geoinf.* 103, 102524. https://doi.org/10.1016/j.jag.2021.102524

Kumar, S., Kumar, D., Chaudhary, S.K., Singh, N., Malik, K.K., 2020. Land subsidence mapping and monitoring using modified persistent scatterer interferometric synthetic aperture radar in Jharia Coalfield, India. *J. Earth Syst. Sci.* 129. https://doi.org/10.1007/s12040-020-01413-0

Prakash, A., Kumar, A., Singh, K.B., 2014. Dynamic Subsidence Characteristics in Jharia Coalfield, India. *Geotech. Geol. Eng.* 32, 627–635. https://doi.org/10.1007/s10706-014-9738-7

Raju, A., Mehdi, K., 2023. SBAS-InSAR analysis of regional ground deformation accompanying coal fires in Jharia Coalfield, India. *Geocarto Int.* 38. https://doi.org/10.1080/10106049.2023.2167004

Riyas, M.J., Syed, T.H., Kumar, H., Kuenzer, C., 2021. Detecting and analyzing the evolution of subsidence due to coal fires in Jharia Coalfield, india using sentinel-1 SAR data. *Remote Sens.* 13, 1–22. https://doi.org/10.3390/rs13081521

Sahu, S.P., Yadav, M., Das, A.J., Prakash, A., Kumar, A., 2017. Multivariate statistical approach for assessment of subsidence in Jharia Coalfields, India. *Arab. J. Geosci.* 10. https://doi.org/10.1007/s12517-017-2985-1

Singh, N., Chatterjee, R.S., Kumar, D., Panigrahi, D.C., 2021. Spatio-temporal variation and propagation direction of coal fire in Jharia Coalfield, India by satellite-based multi-temporal night-time land surface temperature imaging. *Int. J. Min. Sci. Technol.* 31, 765–778. https://doi.org/10.1016/j.ijmst.2021.07.002

Verma, R.K., Bhuin, N.C., Mukhopadhyay, M., 1979. Geology, structure and tectonics of the Jharia Coalfield, India—a three-dimensional model. *Geoexploration* 17, 305–324.